

Measurements of proton-induced radionuclide production cross sections to evaluate cosmic-ray activation of tellurium[#]

A. F. Barghouty¹, C. Brofferio^{2,3}, S. Capelli^{2,3}, M. Clemenza^{2,3}, O. Cremonesi^{2,3}, S. Cebrián⁴, E. Fiorini^{2,3,*}, R. C. Haight⁵, E. B. Norman^{6,7,8}, M. Pavan^{2,3}, E. Previtali^{2,3}, B. J. Quiter⁶, M. Sisti^{2,3}, A. R. Smith⁷, and S. A. Wender⁵

¹ NASA-Marshall Space Flight Center, MSFC, AL 35812 U.S.A.

^{2,3} Dipartimento di Fisica dell' Università di Milano-Bicocca and Istituto Nazionale di Fisica Nucleare Sezione di Milano-Bicocca, 20126 Milan, Italy

⁴ Universidad de Zaragoza, 50009 Zaragoza, Spain

⁵ Los Alamos National Laboratory, Los Alamos, NM 87545 U.S.A.

⁶ Nuclear Engineering Department, University of California, Berkeley, CA 94720 U.S.A.

⁷ Nuclear Science Division, Lawrence Berkeley National Laboratory, Berkeley, CA 94720 U.S.A.

⁸ Physics Division, Lawrence Livermore National Laboratory, Livermore, CA 94551 U. S. A.

* Corresponding author

E-mail address: ettore.fiorini@mib.infn.it

Tel.: 0039 02 64482424 FAX: 0039 02 64482463

[#] [arXiv:1010.4066v1](https://arxiv.org/abs/1010.4066v1)

1 1. INTRODUCTION

2 Experiments designed to study rare events such as the interactions of solar neutrinos [1],
3 dark matter particles [2] or rare processes like double beta decay (DBD) [3] are carried out in
4 underground laboratories. One of the main problems in such searches is the presence in
5 various energy regions of background due to environmental radiation. The contribution due
6 to cosmic rays [4] is strongly reduced by installing the experiment underground [5],
7 sometimes with a further reduction by means of veto counters. While the local environmental
8 radiation, mainly γ -rays or neutrons, can be suitably shielded with inert materials, special
9 care should be devoted to reduce the intrinsic radioactivity of the detector itself or of the
10 material immediately surrounding it [6]. In addition to the natural primordial radioactive
11 contamination of detector material, one has to reduce the presence of radioactive nuclei
12 produced by cosmic rays before the installation underground [7]. Shipping materials by
13 airplane may be an issue due to the much higher cosmic ray flux at high altitude which could
14 be two orders of magnitude higher.

15 The cosmic-ray contribution to the intrinsic radioactivity of detectors has been predicted
16 by various authors using specific codes like COSMO [8] or general purpose codes like
17 GEANT4 [9]. To evaluate the activation cross sections for particles at cosmic ray energies, a
18 set of semi-empirical cross section formulas for proton-nucleus reactions developed by
19 Silberberg and Tsao [10,11], and are used by codes like the mentioned COSMO and the
20 recently introduced ACTIVIA [12]. To improve its reliability, the latter has been tuned to
21 measurements of activation cross sections carried out with protons at various accelerators and
22 can be applied to evaluate the effect of cosmic rays, because the fluxes [4] and cross-sections
23 [12] of cosmic-ray neutrons in altitude can be assumed to be similar to those for protons [13,
24 14]. Many of these cross-section evaluations and measurements have been carried out for
25 germanium [15-25] because of experiments with Ge diodes; others refer to different targets

26 [26-34]. In this paper, we report extensive measurements of proton-induced radionuclide
27 production cross sections on tellurium, for which limited data exist [12,35,36]. The main goal
28 of this study is the identification of the radioactive isotopes that can be produced by cosmic
29 ray exposure of TeO₂ cryogenic detectors (or bolometers) [37].

30 TeO₂ bolometers are used to search for neutrinoless DBD of ¹³⁰Te which has a natural
31 abundance of 33.8 % and a transition energy ($Q_{\beta\beta}$) of 2527.0 keV [38,39]. The best
32 sensitivity on the absolute neutrino mass, comparable to the one of ⁷⁶Ge and ¹⁰⁰Mo
33 experiments, has been reached with the CUORICINO experiment [40,41] based on an array
34 of 62 crystals of TeO₂ with a total mass of about 40.7 kg. To improve this result a larger scale
35 experiment is presently under construction : The Cryogenic Underground Observatory for
36 Rare Events (CUORE) [42,43] will employ approximately 750 kg of TeO₂ bolometers in a
37 search for the neutrinoless DBD of ¹³⁰Te. Its aim is to reach a sensitivity on the absolute
38 neutrino mass as indicated by the results of neutrino oscillations in the inverse hierarchy
39 hypothesis. Minimizing the background in the vicinity of the $Q_{\beta\beta}$ value is crucial for the
40 success of this experiment. Thanks to the deep underground location of the apparatus (that is
41 being assembled in the underground Laboratori Nazionali del Gran Sasso, Italy) and to a
42 careful design of the gamma-ray and neutron shields [44,45], the main background sources in
43 CUORE will come from the radioactivity of the detector constructing materials [42,43,46,47].
44 Among these sources, cosmogenic activated isotopes may play a relevant role. For this reason
45 a special protocol for the crystal procurement have been studied [46,47] in order to minimize
46 the exposure of TeO₂ crystals to cosmic rays during growth and transportation: crystals are
47 delivered from China (where they are grown) to Italy by ship in order to avoid the larger
48 activation due by air transportation, then are immediately stored underground. The total
49 exposure to sea-level cosmic rays does not exceed 45 days (starting from growth) while the
50 storage underground is between 4 and 1 years long, depending on the production batch.

1
2
3
4
5
6
7
8
9
10
11
12
13
14
15
16
17
18
19
20
21
22
23
24
25
26
27
28
29
30
31
32
33
34
35
36
37
38
39
40
41
42
43
44
45
46
47
48
49
50
51 To demonstrate that this procurement protocol is able to ensure acceptable low levels of
52 cosmogenic activation is not straightforward. Indeed, a direct evaluation of the activity of the
53 potentially dangerous isotopes is often impossible: whatever the technique used the sensitivity
54 is too low (as an example CUORE requirements for the TeO₂ crystal contamination in ⁶⁰Co
55 are below one μBq/kg [42]).

56 For this reason the only solution is to rely on the computation of the expected activity on the
57 basis of crystal exposure time, cosmic ray fluxes and activation cross sections.

58 2. EXPERIMENTAL SETUP

59 Exposures to the proton beams of TeO₂ samples have been performed in USA at the Los
60 Alamos National Laboratory's Neutron Science Center at 0.8 GeV and in Europe at CERN at
61 1.4 and 23 GeV. The content of other elements in our samples was always less than a μg/g.
62 Before exposure, each sample was tested for the presence of relevant activities produced by
63 cosmic rays which were found to be negligible. All accelerator activation has been followed
64 by γ-ray spectroscopic analysis of the irradiated samples at different times after irradiation.

65 2.1 MEASUREMENTS CARRIED OUT IN USA

66 The 0.80-GeV irradiation was conducted in the "Blue Room" at the Los Alamos National
67 Laboratory's Neutron Science Center (LANSCE). The Te target was fabricated from
68 99.9999% pure Te Alpha Aesar metallic powder that was pressed into a 6.9-mm thick disk
69 that had 93.4% of normal Te metal density. To confirm that the proton beam was impinging
70 entirely upon the target, a phosphor was placed in the target position before irradiation. A
71 stack of targets was placed in air and irradiated with 800 ± 5 MeV protons for approximately
72 5 minutes. The total beam fluence was monitored by a beam current integrator in order to
73 have approximately 10^{13} protons incident upon the target stack. The stack was made up of
74 6.4 mm thick polyethylene in front of the Te target and then an aluminium backing of 2 mm
75 thickness. More precise proton fluence numbers were extracted from the production of ²²Na

76 and ^7Be in the monitor materials. The proton fluence deduced from the monitor foils was
77 determined to be $(1.2 \pm 0.1) \times 10^{13} \text{ p}\cdot\text{cm}^{-2}$. The cross sections for production of these isotopes
78 from ^{27}Al have been previously determined using a very similar experimental setup at LANL
79 [49], so these cross sections were used instead of evaluated data. The polyethylene monitor
80 was analyzed using evaluated data for the $\text{C}(\text{p}, \text{x})^7\text{Be}$ cross section [50]. It should be noted
81 that the energy lost by protons while traversing the target stack was significantly less than the
82 overall uncertainty in the beam energy and therefore the proton energies are assumed to
83 remain constant throughout the stack.

84 After the bombardment at 0.8 GeV at LANSCE, the samples were transported from Los
85 Alamos back to Lawrence Berkeley National Laboratory (LBNL) where counting began
86 approximately 15 days after irradiation. The samples were initially assayed with a 25%
87 relative efficiency (with respect to that of a 7.62 x 7.62 cm NaI detector) n-type coaxial high-
88 purity germanium detector. The samples were counted multiple times over the course of a
89 week in order to extract half-life information from lines that could not be readily identified.
90 These counting runs occurred at both 7.6 cm from the detector's end cap and with the sample
91 against the end cap. Later, the targets were counted for longer periods with an 80% relative
92 efficiency high purity germanium detector at LBNL's Low Background Facility (LBF). They
93 were counted there intermittently for approximately one year to allow weaker long-lived lines
94 to appear out of the Compton continuum. These counting runs occurred with samples either
95 at 12 cm from the end cap or touching the end cap. All of the measurements of the targets
96 irradiated at LANSCE were performed using ORTEC PC-based data acquisition systems.
97 Figure 1 illustrates an energy spectrum of the Te target taken approximately 16 days after the
98 LANSCE irradiation.

99 To determine the detection efficiencies for the four counting arrangements described
100 above, calibrated point sources of ^{22}Na , ^{54}Mn , ^{57}Co , ^{60}Co , ^{109}Cd , ^{137}Cs , ^{152}Eu and ^{228}Th were

101 used to establish a full-energy efficiency calibration curve of the detectors for point sources.
102 The thick targets that were being counted, however, were sufficiently different from point
103 sources to warrant further effort. In order to establish first-order corrections for both the
104 geometric and self-attenuating effects of the thick targets, an identical un-irradiated Te target
105 (henceforth referred to as “blank”) was placed at the described distance and the point source
106 was placed behind the blank. The efficiency curves resulting from these two geometries were
107 then averaged to produce the effective efficiency curve for a given target being counted by a
108 given detector. While this method proved effective for the calibration of counting geometries
109 where the targets were further from the detector, coincident summing of lines prevented it
110 from being practical when the targets were placed directly against the end caps of the
111 detectors. In this case we employed a method similar to that described by Gmuca and
112 Ribansky [51]. An efficiency curve for a geometry with the source further from the detector
113 is determined as above, then using only the sources with non-coincident lines, ^{57}Co , ^{109}Cd ,
114 ^{137}Cs , and ^{54}Mn , the ratio of efficiencies at the two geometries is determined and a curve is fit
115 to that ratio. Then the longer-distance efficiency curve is multiplied by the aforementioned
116 curve resulting in the final efficiency curve for these close geometries.

117 A brief inspection of the spectra shown in Fig. 1 allows one to gain an idea as to how many
118 lines were present in the spectra. Each line was identified by energy and half-life. Where
119 lines could be attributed to multiple isotopes, other lines were searched for to determine if one
120 could positively identify which isotope was producing the line. If there was no way to
121 confirm the presence of an isotope because it only had a single line or its other lines were also
122 irresolvable, information from the half-life was employed. Cross sections were determined
123 using the extracted γ -ray peak areas, measured γ -ray detector efficiencies, tabulated γ -ray
124 intensities [51], measured target thickness, measured proton fluence and the start and stop
125 times of the γ -ray counting.

126 2. 2 MEASUREMENTS CARRIED OUT IN EUROPE

1
2 127 Crystals of TeO_2 with natural isotopic composition of tellurium [48] were exposed in air to
3
4 128 two proton beams of different energies at CERN. Details on the samples and on the exposures
5
6 129 are reported in Table I. A single exposure of a telluride crystal of 0.457 g mass and irregular
7
8
9 130 shape was performed at the 1.4 GeV beam of ISOLDE using the RABBIT system [52]. The
10
11 131 cross section of the beam was approximately circular with a radius at half maximum of ~ 2
12
13 132 cm, thus totally covering the sample. The geometrical beam profile was taken into account to
14
15 133 evaluate the effective proton fluence on the target. Due to the small thickness of the target,
16
17 134 energy loss in it was negligible. The total beam fluence was monitored by a beam current
18
19 135 integrator and known to within 10%.

20
21
22 136 Two exposures were also carried out in air with the 23 GeV beam at the IRRADIATION 1
23
24 137 Facility at the CERN PS East Hall [53,54]. The beam fluence was monitored with a current
25
26 138 integrator and tested by activation of a 100 μm thick Al foil. The overall uncertainty on the
27
28 139 fluence was 10%. The first exposure was carried out with a crystal of TeO_2 of irregular shape
29
30 140 with a mass of 0.428 g and a low proton fluence in order to pre-evaluate the expected activity
31
32 141 after irradiation. Also in this case the cross section of the beam did totally covered the sample
33
34 142 and the beam profile was used to evaluate the effective proton fluence on the target. The loss
35
36 143 of protons in the crystal is negligible.

37
38
39 144 A second exposure was performed later with a larger TeO_2 crystal of 23 x 22 mm sides and
40
41 145 1.6 mm thickness. As for the exposure at 1.4 GeV, the energy loss of the protons inside the
42
43 146 target was negligible. The cross section of the beam was approximately circular with a radius
44
45 147 at half maximum radius of ~ 8 mm. Since the beam did not cover the entire target the
46
47 148 effective fluence through it was calculated taking into account, also in this case, the beam
48
49 149 profile.

150 For radiation safety reasons and in order to avoid transportation from the irradiation zones,
151 γ -ray spectroscopy for the CERN irradiated samples was first performed for period of a few
152 months after exposure by the Irradiation Facility of CERN with standard CANBERRA Ge
153 spectrometers with relative efficiency of up to 40% (with respect to that of a 7.62 x 7.62 cm
154 NaI detector). However, since the presence of long-living isotopes is more relevant for a low-
155 background underground experiments like CUORE, the sample irradiated at 1.4 GeV and the
156 second one of those irradiated at 23 GeV were shipped to Milan years after the exposure,
157 when the activity due to the short-living isotopes had sufficiently decreased.

158 The irradiated samples were then analyzed with two high purity germanium detectors,
159 one of ~30% and the other one of ~60% relative efficiency. The energy resolutions of the two
160 detectors at 1.33 MeV were 1.77 keV and 2.01 keV FWHM, respectively. All detectors were
161 operated in the low-radioactivity laboratory of the Italian National Institute for Nuclear
162 Physics (INFN) and of the University of Milano-Bicocca in the basement of the Territorial
163 and Environmental Science Department.

164 Monte Carlo simulations were done in order to correctly evaluate the HPGe absolute
165 detection efficiency (ϵ_{abs}) considering the relative position of the samples with respect to the
166 detector. The efficiency of the detector for the analyzed radioisotopes was reconstructed with
167 the aim of evaluate all possible aspects, especially those connected with coincidence summing
168 effect that can influence the full energy peak efficiency for some radionuclides (for example:
169 the complete decay scheme of ^{60}Co , ^{65}Zn , ^{54}Mn , $^{102\text{m}}\text{Rh}$ and $^{110\text{m}}\text{Ag}$ were considered).

170 The software utilized named Jazzy, is based on GEANT4 [9]. This code has been tested by
171 exposing our detectors to several certified gamma ray sources (point like and extended) of the
172 Italian Authority ENEA and found to reproduce the entire spectrum (50 keV up to 2.5 MeV)
173 within 5% error [6]. Taking into account the irregular shape of samples, it was assumed a
174 systematic error of 10% in the overall gamma ray efficiency.

175 The spectra obtained with the γ -ray measurements performed 4.58 and 2.83 years after
176 the exposures at 1.4 and 23 GeV are reported in Figures 2 and 3, respectively. They clearly
177 show the presence of long-living isotopes produced by proton activation. Identifications of the
178 major peaks produced by the irradiation are also indicated (Figures 2b and 3b).

179 3. RESULTS AND DISCUSSION

180 Our primary aim was to determine the production cross sections of long-lived isotopes,
181 such as ^{60}Co , and other long-living nuclei, whose presence could contribute to the background
182 in the energy region of interest (2527 keV in the case of ^{130}Te neutrinoless DBD). The quoted
183 errors (90% c.l.) include in addition to statistics also the uncertainties on proton fluence and
184 detector efficiency. The gamma rays produced by the decay of ^{60}Co in the proton-irradiated
185 Te targets are initially obscured by the activity of short-lived isotopes and can only be reliably
186 measured months or years after the exposures. For completeness, however, we also report our
187 results for relatively short-lived isotopes, which could play a role in the first period of the
188 underground experiment, especially if the material was shipped by airplane.

189 The experimental results obtained from the irradiations performed at LANSCE and CERN
190 are reported in Tables II and III, for long and short-living isotopes, respectively. We have
191 calculated and also reported in the Tables the production cross sections calculated using the
192 latest version of the semi-empirical formulae of Silberberg and Tsao (S&T) [10,11] (using
193 the YIELDX routine). We note that the code only calculates cross sections for a specific
194 daughter to be produced from a specific target. Thus, to determine each production cross
195 section as defined above, calculations must be performed for each naturally occurring target
196 isotope yielding the daughter nuclide as well as all short-lived precursors that decay to the
197 daughter of interest. In the S&T calculations, no discrimination is made between meta-stable
198 and ground states.

199 Before comparing our results with predictions, we would like to stress that the evaluation
200 of Silberberg and Tsao is based on the hypothesis of activation by spallation [55]. This is
201 definitely correct for product nuclei with atomic weight significantly different from those of
202 the isotopes of Tellurium, but not when A is close to them. We found in fact an important
203 presence of the isotopes ^{121}Te , $^{121\text{m}}\text{Te}$, ^{123}Te and ^{129}Te due to the large cross section of thermal
204 neutrons which were present during irradiation. A similar consideration applies to the
205 production of ^{124}Sb , ^{125}Sb , and ^{126}Sb where one can expect a large contribution from (n,p)
206 reactions by fast neutrons on the ^{124}Te , ^{125}Te and ^{126}Te nuclei which have a large isotopic
207 abundance (4.816, 7.14 and 18.95% , respectively). For this reason we have not reported data
208 on the cross section for the production of all these isotopes.

209 We would like to note that for two isotopes, ^{48}V and ^{103}Ru , there is a cumulative effect
210 which could increase the estimated production. In addition to the direct production, ^{48}V is
211 produced by β^+ /EC decays from $^{48}\text{Fe} \Rightarrow ^{48}\text{Mn} \Rightarrow ^{48}\text{Cr} \Rightarrow ^{48}\text{V}$ while ^{103}Ru could be produced
212 by β^- decays from $^{103}\text{Y} \Rightarrow ^{103}\text{Zr} \Rightarrow ^{103}\text{Nb} \Rightarrow ^{103}\text{Mo} \Rightarrow ^{103}\text{Tc} \Rightarrow ^{103}\text{Ru}$. For this reason we
213 have evaluated the expected direct activation cross sections of ^{48}Fe , ^{48}Mn , ^{48}Cr and ^{48}V and
214 sum them to get cumulative cross section for ^{48}V . The same has been done to evaluate the
215 activation cross section for ^{103}Ru . As can be seen from the Tables, the calculated and
216 measured are typically within a factor 2 of each other, as was also reported in previous
217 published paper on proton spallation reactions on Te [35,36]. Larger deviations from the
218 calculated values and the experimentally measured ones are found for different nuclei and for
219 different proton energies by Yu. T. Titarenko et al [29].

220 4. CONCLUSIONS

221 The above reported cross sections can be used to evaluate the contribution by cosmic ray
222 activation of TeO_2 crystals to the background of CUORE. Limiting ourselves to long living
223 nuclei (Table II), the only two isotopes able to contribute to the background in the Region Of

224 Interest (ROI) for the ^{130}Te Double Beta Decay study are ^{60}Co and $^{110\text{m}}\text{Ag}$. Indeed all the
225 others have a maximum energy release in the crystal far below the ROI. A rough evaluation
226 of the initial activity of these isotopes in TeO_2 crystals is obtained using the cross sections
227 reported in Table II and binning the cosmic ray spectrum at sea level accordingly. For an
228 average exposure of 45 days, we obtain an activity of about 2×10^{-8} Bq/kg in ^{60}Co and 4×10^{-6}
229 Bq/kg in $^{110\text{m}}\text{Ag}$. These activities will decrease before the start of the experiment (the storage
230 time varies between 5 and 1 years depending on the crystal production batch) by a factor 2
231 (for ^{60}Co) and 9 (for $^{110\text{m}}\text{Ag}$) leading to a global contribution in the ROI that – according to
232 preliminary evaluations - is at least one order of magnitude below the target counting rate for
233 CUORE.

234 ACKNOWLEDGMENTS

235 We would like to express our gratitude to the ISOLDE Collaboration and in particular to
236 Alexander Helert and Ulli Koester and to the ISOLDE Technical group for assistance and
237 support. We are also grateful to the CERN IRRADIATION FACILITY and in particular to
238 Maurice Glaser for help and advice in the exposures at 23 GeV. This work was supported in
239 part by the U. S. Department of Energy under contract numbers DE-AC52-07NA27344 at
240 LLNL and DE-AC02-05CH11231 at LBNL.

241 REFERENCES

- 242 [1] W. C. Haxton, arXiv:0808.0735 and Encyclopedia of Applied High Energy and Particle
243 Physics (ed. R Stock) (2008) 221.
244 [2] L. Baudis, arXiv:0711.3788v1 and Proc. SUSY07 (Karlsruhe, 2007) 198.
245 [3] F. T. Avignone III, S. R. Elliott, J. Engel, Rev. Mod. Phys. **80** (2008) 481.
246 [4] C. Amsler, et al., Review of Particle Physics, Phys. Lett. B **667** (2008) 1.
247 [5] S. Niese, Radioactivity in the Environment **11** (2008) 209.
248 [6] C. Bucci et al. , Eur. Phys. Journal A 41(2009) 155.

- 249 [7] G. Heusser, Annual. Rev. Nucl. Part. Sci. **45** (1995) 543.
- 1
2 250 [8] C. J. Martoff and P.D. Lewin, Comp. Phys. Commun. **72** (1992) 96.
- 3
4 251 [9] S. Agostinelli et al, Nucl. Instr. and Meth. A **506** (2003) 250.
- 5
6 252 [10] R. Silberberg, C.H. Tsao, Astrophys. J. Suppl. **220** (I) (1973) 315; Astrophys. J. Suppl.
- 7
8
9 253 **220** (II) (1973) 335; Physics Reports **191** (1990) 351.
- 10
11 254 [11] R. Silberberg, C.H. Tsao and A.F. Barghouty. Astrophys. J. **501** (1998) 911.
- 12
13 255 [12] J. J. Back and Y. A. Ramachers: Nucl. Instrum. Meth. A **586** (2008) 286-294.
- 14
15 256 [13] X. Hou, Radioactivity in the Environment, **11** (2008) 371.
- 16
17 257 [14] G. Heusser, M. Laubenstein, H. Neder, Radioactivity in the Environment, **8** (2006) 495.
- 18
19 258 [15] I. Barabanov et al., Cosmogenic activation of Germanium and its reduction for low
- 20
21 259 background experiments, nucl-ex/0511049 (2005) and Radioactivity (2007) 1. Nucl.
- 22
23 260 Instrum. Meth. B **251** (2006) 115-120.
- 24
25
26 261 [16] H. Gómez, S. Cebrián, J. Morales, J.A. Villar, Astropart. Phys. **28** (2007) 435.
- 27
28
29 262 [17] S. Fiorucci et al, Astropart. Phys. **28** (2007) 143.
- 30
31
32 263 [18] F. T. Avignone et al., Nucl. Phys. B Proc. Suppl. **28** (1) (1992) 280.
- 33
34
35 264 [19] M. Blann, Phys. Rev. C **54** (1996) 1341; M. Blann, M.B. Chadwick, Phys. Rev. C **57**
- 36
37 265 (1998) 233.
- 38
39
40 266 [20] H. V. Klapdor-Kleingrothaus, et al., Nucl. Instr. and Meth. A **481** (2002) 149.
- 41
42
43 267 [21] H. S. Miley, et al., Nucl. Phys. B Proc. Suppl. **28** (I) (1992) 212.
- 44
45
46 268 [22] D. M. Mei, Z. . Yin, S. R. Elliott Astropart. Phys. **31** (2009) 417-420.
- 47
48
49 269 [23] Mei, D.M.; Elliott, S. R.; Hime, A., et al. , Phys. Rev. C **77** (2008) 054614.
- 50
51 270 [24] S. R. Elliott et al., Phys. Rev. C **82** (2010) 054610.
- 52
53 271 [25] A study on activation in germanium by neutrons due to muon interactions underground is
- 54
55 272 reported in D. M. Mei and A. Hime: Muon-induced background study for underground
- 56
57 273 laboratories, astro-ph/0512125 6 Dec. 2005 Phys. Rev. D **73** (2006) 053004.
- 58
59
60
61
62
63
64
65

- 274 [26] J. A. Formaggio, C. J. Martoff, *Ann. Rev. Nucl. Part. Sci.* **54** (2004) 361.
- 1
2
3 275 [27] E. Porras et al, *Nucl. Instr. and Meth. B* **160** (2000) 73.
- 4
5 276 [28] Yu. E. Titarenko et al., *Phys.Rev. C* **78** (2008) 034615.
- 6
7 277 [29] Yu. E. Titarenko et al.: Verification of high-energy transport codes on the basis of
8
9
10 278 activation data arXiv:1106.0054.
- 11
12 279 [30] S. Takaca et al., *Nucl. Instr. and Meth. B* **188** (2002) 106.
- 13
14 280 [31] S. Takaca et al., *Nucl. Instr. and Meth. B* **251** (2006) 56.
- 15
16
17 281 [32] L. Baudis and R.W. Schnee, Dark Matter experiments, NUSL White Paper, 2002.
- 18
19 282 [33] A. C. Rester et al., *Nucl. Instr. and Meth. A* **297** (1990) 258.
- 20
21
22 283 [34] V. E. Giuseppe, M. Devlin, S. R. Elliott, et al., *Physical Review C* **79** (2009) 054604.
- 23
24 284 [35] D.W. Bardayan et al., *Phys. Rev. C* **55** (1997) 820.
- 25
26
27 285 [36] E.B. Norman et al, *Nucl. Phys. B (Proc.Suppl.)* **143** (2005) 508.
- 28
29 286 [37] N. Booth, B. Cabrera and E. Fiorini, *Ann. Rev. Nucl. Part. Sci.* 46(1996) 471; C. Enns
30
31
32 287 and D. McCammon, *J. Low Temp.Phys* 151 (2008) 5.
- 33
34 288 [38] N. D. Scielzo et al., *Phys. Rev. C* **80** (2009) 025501.
- 35
36
37 289 [39] M. Redshaw et al., *Phys. Rev. Lett.* **102** (2009) 212502.
- 38
39 290 [40] E. Andreotti et al, *Astropart. Phys.* 34 (2011) 822
- 40
41 291 [41] C. Arnaboldi et al., *Phys. Rev. C* 78 (2008) 035502
- 42
43
44 292 [42] C. Arnaboldi et al., *Nucl. Instrum. & Meth. A* **518** (2004) 775.
- 45
46 293 [43] M. Pedretti et al., *International Journal of Modern Physics A.* 23 (2008) 3395.
- 47
48
49 294 [44] F. Bellini et al., *Astroparticle Physics* 33 (2010) 169.
- 50
51 295 [45] E. Andreotti et al., *Astroparticle Physics* 34 (2010) 18.
- 52
53
54 296 [46] F. Alessandria et al., *Astroparticle Physics* 35 (2012) 839.
- 55
56 297 [47] M. Pavan et al., *Eur. Phys. Journal A* 36 (2008) 159
- 57
58 298 [48] C. Arnaboldi et al. *Journal of Crystal Growth* 312 (2010) 2999.
- 59
60
61
62
63
64
65

299 [49] T. N. Taddeucci et al., Phys. Rev. C **55** (1997) 1551.

300 [50] J. B. Cumming, Ann. Rev. of Nuc. and Part. Sci. Vol. **13** (1963) 261.

301 [51] S. Gmuca, S. and I. Ribansky, Nucl. Instr. and Meth. **202** (1982) 435.

302 [52] E. Kugler , Hyperfine Interactions **129** (2000) 23.

303 [53] M. Moll and M. Glaser: Proton and neutron irradiation facilities in the CERN East Hall-

304 EP common project , presented to the EP Technical Coordinator meeting on 23.9.2002.

305 [54] M. Glaser et al., Nucl. Instr. and Meth. A **426** (1999).

306 [55] M. N. Andronenko, L. N. Andronenko and W. Neubert , Eur. Phys.J. A **31** (2007) .

ACCEPTED MANUSCRIPT

Proton Energy (GeV)	Fluence (p/cm ²)	Mass TeO ₂ (g)	Mass Te (g)	Delay Time (h)	Measurement Live Time (s)
1.4 (a)	1.5 x 10 ¹⁵	0.457	0.365	1240.5	297022
1.4 (b)	1.5 x 10 ¹⁵	0.457	0.365	4827.5	251358
1.4 (c)	1.5 x 10 ¹⁵	0.457	0.365	40124.5	583178
23 (0)	9.41 x 10 ¹⁰	0.424	0.339	848.2	50400
23 (a)	6.1 x 10 ¹²	51.11	40.9	2224	1097
23 (b)	6.1 x 10 ¹²	51.11	40.9	2591	50400
23 (c)	6.1 x 10 ¹²	51.11	40.9	13606	200000
23 (d)	6.1 x 10 ¹²	51.11	40.9	24793	861228

TABLE 1. CERN Irradiations data and delay and live times of Gamma ray spectrometry measurements

Isotope	Half Life (d)	Gamma Ray Energy (keV)	Decay Mode	σ Expt. 0.8 GeV (mb)	σ S&T 0.8 GeV (mb)	σ Expt. 1.4 GeV (mb)	σ S&T 1.4 GeV (mb)	σ Expt. 23 GeV (mb)	σ S&T 23 GeV (mb)
⁵⁴ Mn	312	1377	EC	0.04±0.02	0.11		0.40	1.5±0.3	4.0
⁵⁷ Co	272	836	EC	0.05±0.01	0.20	0.15±0.05	0.73	0.87±0.09	1.1
⁶⁰ Co	1923.6	2824	β^-	0.09±0.04	0.22	0.20±0.04	0.77	0.75±0.08	1.15
⁶⁵ Zn	244	1352	EC, β^+	0.11±0.02	0.46	1.2±0.3	1.5	1.8±0.2	2.4
⁷⁵ Se	120	864	EC	0.26±0.08	1.1	3.2±0.3	2.7	3.1±0.3	4.3
⁸⁸ Y	107	3623	EC, β^+	3.1±1.2	1.3	4.6±0.8	5.0	4.2±0.6	3.1
¹⁰² Rh	207	2323 1151	EC, β^+ β^-	4.9±1.2	7.9	1.5±0.3	11		5.8
^{102m} Rh	1058.5	2323	EC, β^+	4.0±0.6	1.3	2.4±0.5		1.5±0.2	
^{110m} Ag	250	2892	β^-	24.6±3.7	16.0	1.9±0.3	1.2	0.88±0.59	0.64
¹¹³ Sn	115	1036	EC	12.4±1.9	19.5	27±5	19		11

TABLE 2. Results for activation of isotopes with half life > 100 days

Isotope	Half Life (d)	Gamma Ray Energy (keV)	Decay Mode	σ Expt. 0.8 GeV (mb)	σ S&T 0.8 GeV (mb)	σ Expt. 1.4 GeV (mb)	σ S&T 1.4 GeV (mb)	σ Expt. 23 GeV (mb)	σ S&T 23 GeV (mb)
⁴⁶ Sc	83.8	2367	β^-	0.05±0.01	0.11		0.29	1.5±0.3	2.9
⁴⁸ V	16	4012	EC, β^+				0.12	24±5	1.2
⁵⁶ Co	77.3	4566	EC, β^+	0.10±0.02	0.18		0.04	0.18±0.03	0.40
⁵⁸ Co	70.9	2307	EC, β^+	0.04±0.01	0.38	0.5±0.1	1.45	1.7±0.3	2.2
⁵⁹ Fe	44.5	1565	β^-			0.3±0.1	0.20	0.74±0.17	0.47
⁸³ Rb	86.2	909	EC	1.6±0.2	2.6		4.1	5.3±0.8	3.8
⁸⁴ Rb	32.8	2681	EC, β^+	0.40±0.06	0.4	4.8±0.8	1.7	4.2±0.7	1.6
⁸⁵ Sr	64.8	1065	EC	2.1±0.3	3.1		6.1	5.4±0.9	4.8
⁸⁸ Zr	83.4	673	EC				7.0	2.8±0.6	4.2
⁸⁷ Y	3.3	1862	EC, β^+	2.9±0.4	3.2				
⁹⁵ Nb	34.97	926	β^-				1.2	1.5±0.5	0.58
⁸⁹ Zr	3.3	2833	EC, β^+	3.6±0.5	4.7				
^{92m} Nb	10.2	2006	EC, β^+	0.23±0.03	3.6				
⁹⁵ Nb	34.97	926	β^-	0.85±0.17	0.5				
^{95m} Tc	61	1691	EC, β^+	0.46±0.07	7.6				
¹⁰⁰ Pd	3.6	361	EC	6.4±1.1	2.7				
¹⁰³ Ru	39.3	763	β^-	1.4±0.2	0.6		0.82	19±3	0.37
¹⁰⁵ Ag	41.3	1345	EC	10.1±1.7	19.7		15	3.7±1	9.3
¹¹¹ In	2.8	865	EC	16.4±3.0	30.4				
^{114m} In	49.5	1452	EC, β^+	11.6±2.3	3.7	9.2±0.9	3.1	8.0±1,2	1.9

TABLE 3. Results for activation of isotopes with half life < 100 days

FIGURES

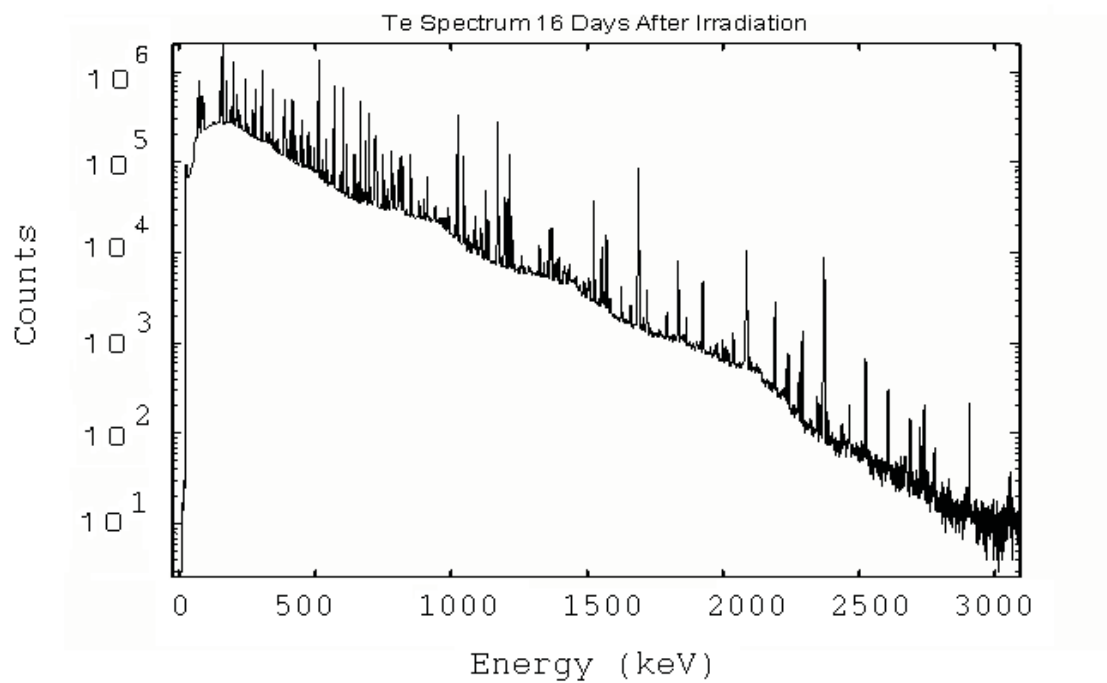


FIGURE 1: γ -ray spectrum recorded 16 days after the LANSCE irradiation with 0.80 GeV protons.

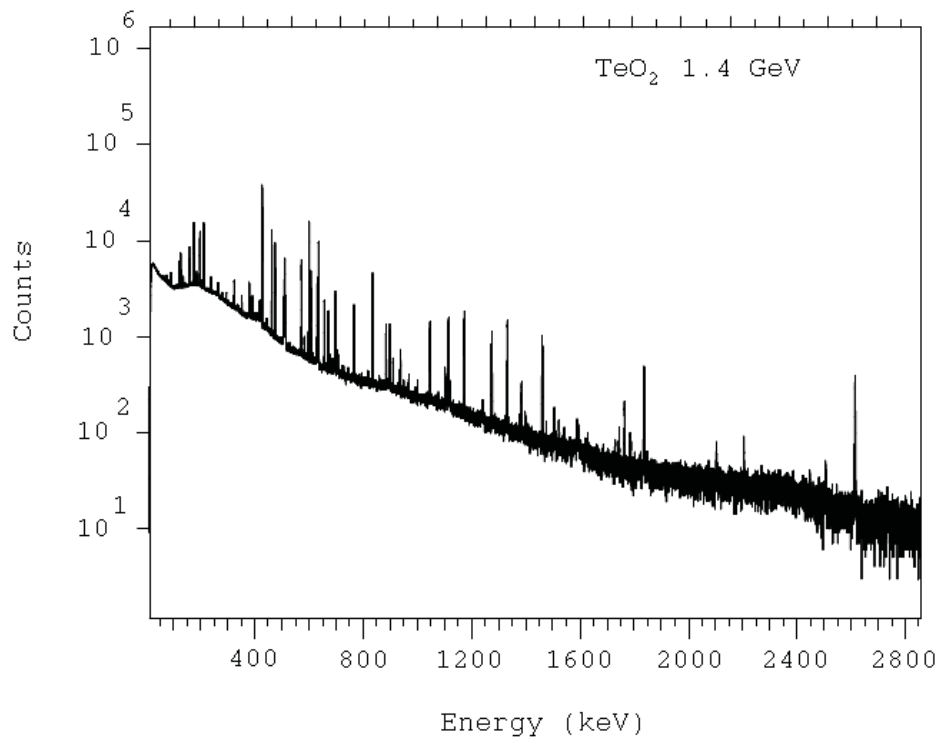


FIGURE 2(a): γ -ray spectrum (583178 sec live time) recorded for the sample irradiated at 1.4. GeV 4.58 years after irradiation: complete spectrum

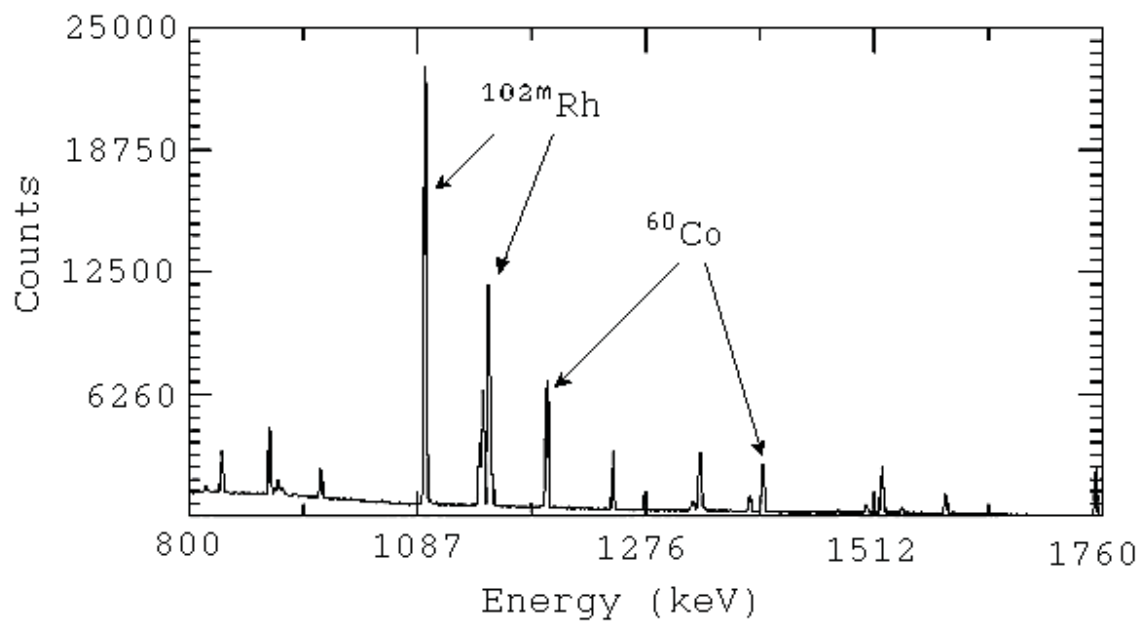


FIGURE 2(b): γ -ray spectrum (583178 sec live time) recorded for the sample irradiated at 1.4. GeV 4.58 years after irradiation: peaks of interest.

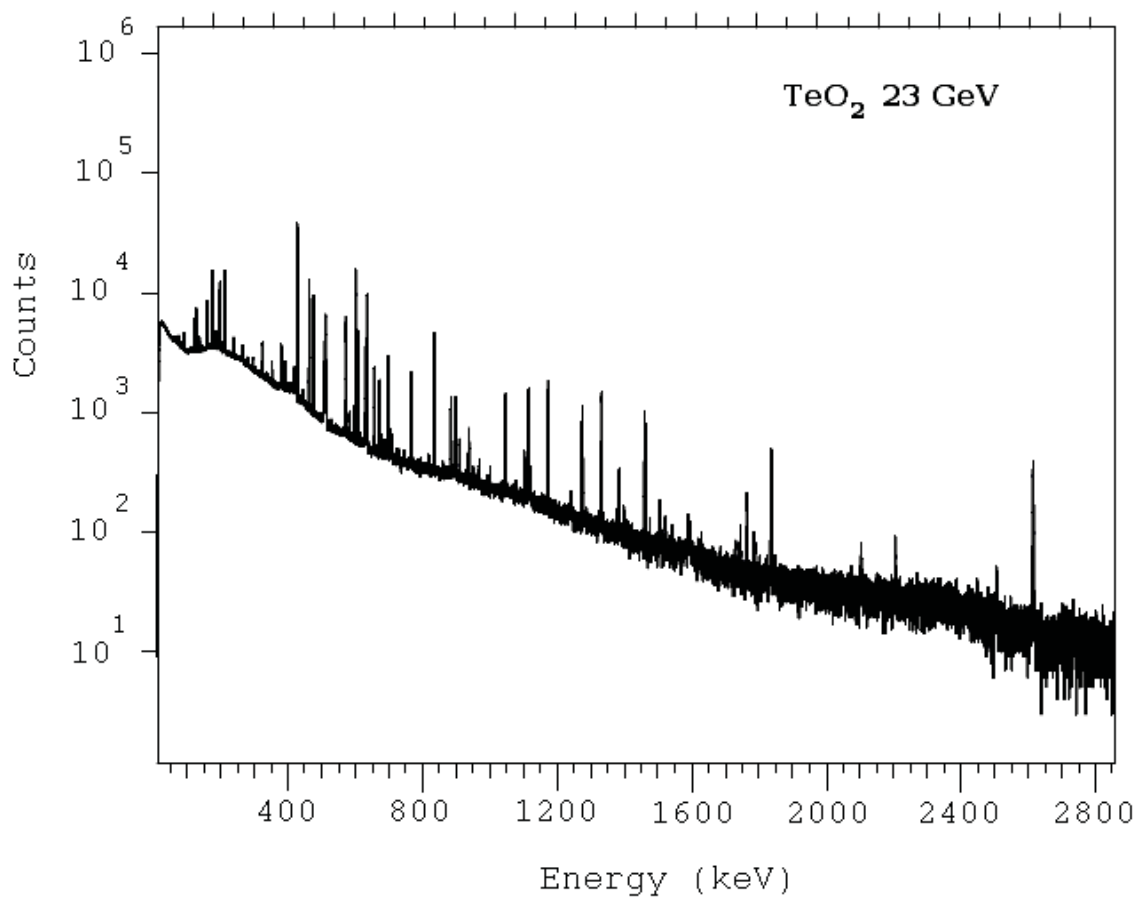


FIGURE 3(a): γ -ray spectrum (861228 sec live time) recorded for the sample irradiated at 23 GeV 2.83 years after irradiation: complete spectrum;

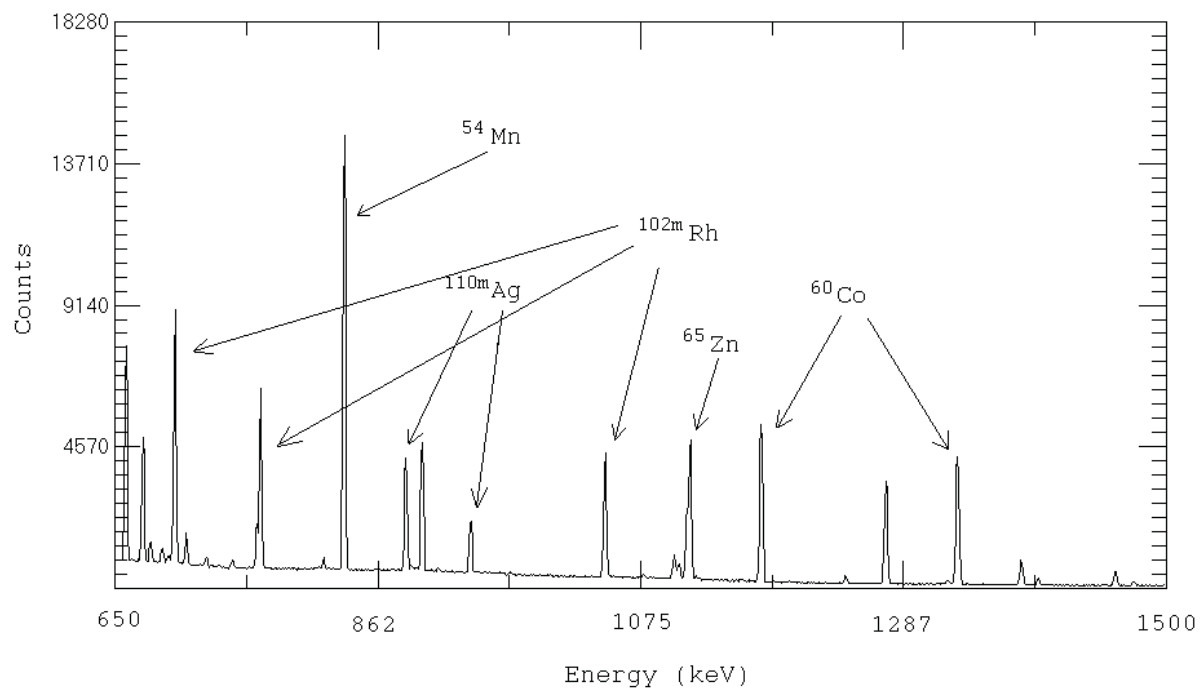


FIGURE 3(b): γ -ray spectrum (861228 sec live time) recorded for the sample irradiated at 23 GeV 2.83 years after irradiation: peaks of interest